CHEMISTRY
A EUROPEAN JOURNAL

DOI: 10.1002/chem.200801803

Equilibrium and Kinetic Properties of the Lanthanoids(III) and Various Divalent Metal Complexes of the Heptadentate Ligand AAZTA**

Zsolt Baranyai,[a, b] Fulvio Uggeri,[c] Giovanni B. Giovenzana,[d] Attila Bényei,[e] Ernő Brücher,[b] and Silvio Aime*[a]

Abstract: The heptadentate ligand 1,4-bis(hydroxycarbonylmethyl)-6-[bis(hydroxycarbonylmethyl)]amino-6-methylperhydro-1,4-diazepine (AAZTA) and its derivatives were recently reported to give stable complexes with Gd^{3+} with superior efficiency as MRI contrast agents. Nevertheless, only preliminary data are available on the coordination behavior of this interesting ligand. In this work, thermodynamic and kinetic stability data are determined for the formation of complexes with AAZTA and the lanthanoid metal ions, and other divalent metal ions of interest for this application. The AAZTA ligand binds the lanthanoid ions with $\log K_{ML}$ values of 17.53–21.85 with its affinity steadily increasing from La^{3+} to Lu^{3+}, suggesting that the seven-membered skeleton is better suited to accommodate smaller metal ions. Even though the denticity is lower, the stability of the heavier lanthanoid complexes is comparable to those of the classical ligand diethylenetriaminepentaacetic acid (DTPA). The transmetalation reactions of $[Gd(AAZTA)]^-$ with Cu^{2+} and Eu^{3+} predominantly occur through proton-assisted dissociation of the complex. The role of the direct attack of Cu^{2+} or Eu^{3+} in the exchange reactions is limited, although the formation of dinuclear complexes decreases the proton-assisted dissociation. Near physiological conditions, $[Gd(AAZTA)]^-$ is significantly more inert than $[Gd(DTPA)]^{2-}$, allowing its potentially safe use as contrast agent in magnetic resonance imaging.

Keywords: kinetics · lanthanides · ligand effects · N ligands · thermodynamics

Introduction

The rich variety of magnetic, optical, and radiochemical properties associated with the metal ions in the lanthanoid series is the reason for the large number of applications of lanthanoid complexes in several areas of chemistry, biology, medicine, and material science.[1] Modulation of these properties may be obtained by carefully tuning the structures of the complexes as a result of the metal ion characteristics and those of the ligands employed in the formation of the complexes.

The advent of magnetic resonance imaging (MRI) as a primary diagnostic technique in clinical practice,[2] enhanced by the use of gadolinium(III) complexes as contrast agents,[3] boosted the study of lanthanoid(III) complexes over the last two decades. More recently, nuclear medicine is also showing a growing interest in lanthanoid chelates for both molecular imaging and therapeutic applications.[4]

Highly stable complexes are needed for in vivo applications to avoid problems associated to the release of toxic metal ions. Recent reports outlined the development of a Gd^{3+} related pathology (nephrogenic systemic fibrosis/nephrogenic fibrosing dermopathy or NSF/NFD) in patients with

[a] Dr. Zs. Baranyai, Prof. S. Aime
Department of Chemistry IFM & Molecular Imaging Center
Università degli Studi di Torino, Via P. Giuria 7, 10125 Torino (Italy)
Fax: (+39) 11-6707521
E-mail: silvio.aime@unito.it

[b] Dr. Zs. Baranyai, Prof. E. Brücher
Department of Inorganic and Analytical Chemistry
University of Debrecen, 4010, Debrecen
Egyetem tér 1. (Hungary)

[c] Dr. F. Uggeri
Bracco Imaging s.p.a., Via E. Folli 50, 20135 Milano (Italy)

[d] Prof. G. B. Giovenzana
DiSCAFF & DFB Center
Università degli Studi del Piemonte Orientale "A. Avogadro"
Via Bovio 6, 28100 Novara (Italy)

[e] Dr. A. Bényei
Department of Physical Chemistry, University of Debrecen
4010, Debrecen, Egyetem tér 1. (Hungary)

[**] AAZTA = 1,4-bis(hydroxycarbonylmethyl)-6-[bis(hydroxycarbonylmethyl)]amino-6-methylperhydro-1,4-diazepine

Supporting information for this article is available on the WWW under http://dx.doi.org/10.1002/chem.200801803.

renal failure as a result of the slow dissociation of some acyclic, Gd^{3+}-containing MRI contrast agents.[5] Clearly these findings indicate the need for the design of more stable complexes for use in these applications. The efficiency of a Gd^{3+} chelate as an MRI contrast agent essentially relies on the number of water molecules coordinated to the paramagnetic metal ion and this is, in general, in contrast to the need to use high denticity ligands to obtain the highest stabilities. Gadolinium(III) complexes derived from macrocyclic (DOTA-like, DOTA = 1,4,7,10-tetraazacyclododecane-1,4,7,10-tetraacetic acid) and acyclic (DTPA-like, DTPA = diethylenetriaminepentaacetic acid) octadentate ligands cover the whole market of this class of clinically approved MRI contrast agents. These systems contain only one coordinated water molecule to give them a limited ability in enhancing the relaxation rate of water protons. Therefore, there is an active search for sufficiently stable Gd^{3+} chelates containing more than one water molecule in the inner coordination sphere of the paramagnetic metal ion. There are few ligands that provide a good compromise between stability and enhanced hydration of the resulting Gd^{3+} complexes; some examples are the hydroxypyridinone (HOPO) family developed by Raymond et al.,[6,7,8] the N-alkyldiethylenetriaminetetraacetic acids reported by the groups of Caravan[9] and Merbach[10] and the AAZTA derivatives (AAZTA = 1,4-bis(hydroxycarbonylmethyl)6-[bis(hydroxycarbonylmethyl)]amino-6-methylperhydro-1,4-diazepine) prepared by our group.[11]

In complexes containing AAZTA, the ligand wraps around the Gd^{3+} ion, yielding a system containing two coordinated water molecules in fast exchange with the "bulk water" solvent. This gives $[Gd(AAZTA)]^-$ a relaxivity that is approximately 40% higher than that of the clinically used agents. More importantly, when $[Gd(AAZTA)]^-$ is bound to a slow-moving substrate, due to the short lifetime of the coordinated water molecules, very high relaxivities can be attained. This was the case of a $[Gd(AAZTA)]^-$ complex with a long aliphatic chain,[12a] which generated a supramolecular adduct with human serum albumin, displaying the highest relaxivity (ca. 80 $mM^{-1}s^{-1}$) reported to date for this class of Gd^{3+}-based contrast agents. The same lipophilic $[Gd(AAZTA)]^-$ system displayed very good relaxation-enhancing properties when bound to low-density lipoproteins[12b] as well as when used as spontaneously formed micelles in cellular labeling experiments.[13] These promising properties prompted us to explore, in detail, the coordination behavior of this interesting new ligand towards lanthanoid ions and other metal ions present in body fluids.

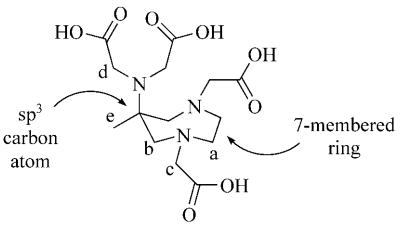

AAZTA

Scheme 1. The ligand AAZTA.

Results and Discussion

Solution equilibria of the AAZTA ligand: The structure of AAZTA (Scheme 1) is designed to form five-membered chelate rings with all nitrogen atoms and to reduce the intramolecular mobility due to conformational motion. The conformational locks are represented by 1) the seven-membered ring, containing two nitrogen atoms, which is sized to avoid extensive flexibility and strong transannular interactions; 2) the sp^3 central carbon of the propylene endocyclic moiety, on which the third nitrogen atom is inserted (its configurational stability precludes undesired extension of the compact coordination set). The AAZTA ligand does not belong to either the traditional categories of acyclic (e.g., ethylenediaminetetraacetic acid (EDTA), DTPA) and macrocyclic ligands (e.g., DOTA), or to other subclasses, such as polypodal ligands (e.g., HOPOs). The presence of the seven-membered ring containing two coordinating nitrogen atoms and with an additional coordinating exocyclic nitrogen atom closely resembles the structural features of lariat ethers, bringing this entry into a scarcely explored class of polyaminocarboxylic ligands.

Intravenously administered metal complexes enter into a number of equilibria with a large variety of species present in body fluids, including several metal ions and ligands.[14,15] Simplified models were proposed to predict the concentration of the free Gd^{3+} in blood plasma in the presence of gadolinium-based MRI contrast agents.[16,17,18] For such equilibrium calculations, it is necessary to know the protonation constants of the ligand, and the composition of the complexes participating in the equilibria, as well as their protonation and stability constants.

The H_4AAZTA ligand may be regarded as a combination of the known ligands DACHDA (H_2DACHDA = 1,4-diazacycloheptane-1,4-diacetic acid) and IMDA (H_2IMDA = imino-*N*,*N*-diacetic acid);[19,20] the IMDA ligand is linked to the central carbon atom. Upon complex formation, the three nitrogen atoms and the oxygen atoms of the four carboxylate groups wrap around the metal ion, the ligand structure providing a relatively flexible preformed coordination cage. Taking into account these considerations, the AAZTA ligand belongs to a new class of the polyaminopolycarboxylic acids showing unique complexation properties.

Protonation equilibria of the AAZTA ligand: The complexation properties and protonation equilibria of H_4AAZTA have not been studied in detail previously.[11] The protonation constants of the ligand, defined by Equation (1), have been determined by pH potentiometry and the $\log K_i^H$ values are listed in Table 1 (standard deviations are shown in parentheses).

Table 1. Protonation constants of the ligands H_4AAZTA and H_5DTPA (25 °C).

	H_4AAZTA					H_5DTPA[a]
	0.1 M KCl	1.0 M KCl	0.1 M KNO_3	0.1 M $(Me)_4NCl$	0.1 M KCl[b]	0.1 M KCl
$\log K_1^H$	11.23 (0.01)	10.93 (0.01)	11.18 (0.01)	11.35 (0.01)	11.16 (0.02)	10.41
$\log K_2^H$	6.52 (0.01)	6.65 (0.01)	6.50 (0.01)	6.61 (0.01)	6.46 (0.02)	8.37
$\log K_3^H$	3.78 (0.01)	3.75 (0.01)	3.78 (0.01)	3.89 (0.01)	–	4.09
$\log K_4^H$	2.24 (0.01)	2.01 (0.01)	2.22 (0.01)	2.40 (0.02)	–	2.51
$\log K_5^H$	1.56 (0.01)	–	1.68 (0.01)	2.12 (0.02)	–	2.04
$\Sigma \log K_i^H$	25.33	23.34	25.36	26.37	–	27.42

[a] Ref. [19]. [b] Obtained by ^1H NMR titration.

$$K_i^H = \frac{[H_iL]}{[H_{i-1}L][H^+]} \qquad i = 1-5 \tag{1}$$

The protonation constants of AAZTA obtained in an aqueous solution of KCl are lower than those obtained in an aqueous solution of $(Me)_4NCl$, indicating the complexation of K^+ with AAZTA. The stability constant of the $[K(AAZTA)]^{3-}$ complex was determined in an aqueous solution of $(Me)_4NCl$. A 0.002 M solution of H_4AAZTA was titrated with $(Me)_4NOH$ in the presence of 0.08 M $(Me)_4NCl$ and 0.02 M KCl. The stability constant of the complex $[K(AAZTA)]^{3-}$ is $\log K_{KAAZTA} = 1.3$ (0.02).

The protonation constants of AAZTA were also determined by measuring the pH-dependent ^1H NMR chemical shifts of the nonlabile protons. The ^1H NMR titration curve (Figure 1) displays sharp changes at different pH values, which are related to the protonation of the ligand. Since the protonation/deprotonation steps of the ligand are fast on the NMR timescale, the chemical shifts of the observed signals represent a weighted average of the shifts of the different species involved in a specific protonation step, as shown in Equation (2):[21]

$$\delta_{H(obs)} = \sum \chi_i \delta_H^{H_iL} \tag{2}$$

in which $\delta_{H(obs)}$ is the observed chemical shift of a given signal, and χ_i and $\delta_H^{H_iL}$ are the molar fraction and the chemical shift of the involved species, respectively. The observed chemical shifts ($\delta_{H(obs)}$) were fitted with Equation (2) (the molar fractions χ_i of the different protonated species were expressed by using the related protonation constants K_i^H). The fit of the experimental data points to the calculated ones is excellent (Figure 1) and the obtained $\log K_i^H$ values are listed in Table 1.

The protonation sequence of AAZTA was assessed on the basis of the pH dependence of the ^1H NMR chemical shifts. Since AAZTA can be regarded as a derivative of DACHDA, the chemical shift of the methylene protons could be assigned with the help of the ^1H NMR spectra of $H_2DACHDA$.[20] The ^1H NMR spectrum of the AAZTA displays a number of signals, particularly at pH > 10 (Figure 1A). The methylenic protons of the ring (labeled a, b in Figure 1A) give rise to two resolved multiplets (a) and an AB system (b), while the protons of the lateral acetate groups (c) generate another AB system. The signals of the acetate methylene protons (d) of the IMDA moiety and of the methyl protons (e) both resonate as singlets. When present as the K^+ complex, the observed signals are the weighted result of the fast exchange between $[K(AAZTA)]^{3-}$ and the different protonated forms of AAZTA that occur according to the pH of the solution.

Starting from basic pH values, the addition of one equivalent of acid to $AAZTA^{4-}$ resulted in a significant downfield shift of the signals of each methylene proton, which indicated that the first protonation takes place at the nitrogen atoms of the ring and the pendant arm (the protonation occurs partially at a ring nitrogen atom and at the IMDA nitrogen atom). In the pH range 5–8, the signals of

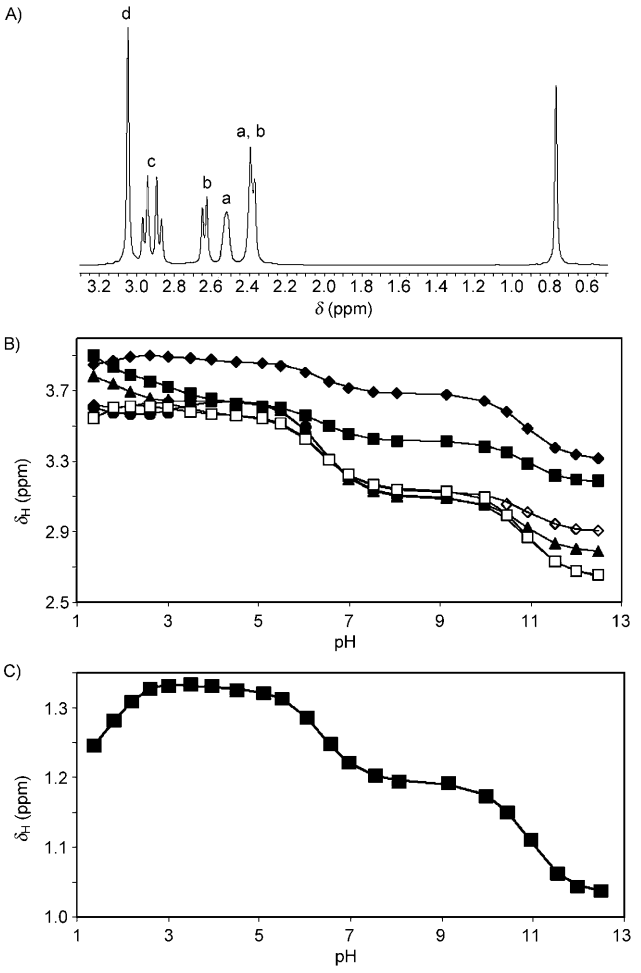

Figure 1. The ^1H NMR spectrum at pH 11.7 (A) and titration curves of the H_4AAZTA ligand (B): a1 (▲), a2 (●), b1 (◇), b2 (□), c (■), d (◆) and (C): e (■); 0.1 M KCl, 25 °C). The symbols are experimentally observed data, and all lines are calculated.

the methylene protons of the ring are mainly affected by the second protonation process, which occurs at a nitrogen atom of the ring.[20] In the same pH range, however, the signal of the methylene protons of the IMDA group also shifts to slightly higher frequencies (downfield), suggesting that, concomitant to protonation of the ring nitrogen, the first proton is transferred to the nitrogen of the IMDA group as a consequence of the electrostatic repulsion between the protonated nitrogen atoms of the ring. Further lowering of the pH resulted in the downfield shift of the signals corresponding to the methylene protons of the ring acetates between pH 3 and 4.5, confirming that the $\log K_3^H$ is related to the protonation of the carboxylate groups bound to the nitrogen atoms of the ring. Finally, the last protonations occur at the non-protonated nitrogen atom of the ring and the carboxylate pendant arms. The values of $\log K_1^H$ and $\log K_2^H$ obtained from the ^{1}H NMR spectroscopic studies are in good agreement with the data determined by pH potentiometry. The protonation sites of AAZTA found by ^{1}H NMR spectroscopy are in agreement with by the solid-state structure of the H_4AAZTA ligand.[22]

Complexation properties of the AAZTA ligand: A comparison of the protonation constants of AAZTA and DTPA obtained in similar media reveals that $\log K_3^H$ and $\log K_4^H$ values are similar, whereas the $\log K_1^H$ and $\log K_2^H$ values are different. The first protonation constant of the AAZTA is somewhat higher, whereas the second protonation constant is lower by 1.5 $\log K$ units than that of DTPA. The $\Sigma \log K_i^H$ values, presented in Table 1, indicate that the total basicity of AAZTA is somewhat lower than that of DTPA. It is generally accepted that nonionic donor atoms are bound more weakly to Ln^{3+} ions than anionic donor atoms; the number and the type of the donor atoms therefore have an important role in the stability of Ln^{3+} complexes formed with polyaminopolycarboxylate ligands. By taking into account the lower basicity and denticity of AAZTA, the stability constant of the Ln^{3+} complexes of AAZTA are expected to be somewhat lower than those of DTPA. In determining the stability constants of the AAZTA complexes, the size match between the metal ion and the flexible coordination cage formed by complexation, may also play an important role. Therefore, the equilibrium study of the metal complexes formed with AAZTA may give some new information about the interaction between the metal ions and the heptadentate ligand and also on the effect of the formation of the coordination cage on the thermodynamic stability.

The stability and protonation constants of the metal complexes formed with the AAZTA ligand are defined by Equations (3) and (4):

$$K_{ML} = \frac{[ML]}{[M][L]} \tag{3}$$

$$K_{MH_iL} = \frac{[MH_iL]}{[MH_{i-1}L][H^+]} \qquad i = 1, 2 \tag{4}$$

The stability constants obtained by pH potentiometric titrations (or by UV/Vis spectrophotometric techniques for the Cu^{2+} complex) are reported in Table 2.

Table 2. Protonation and stability constants of metal complexes of the ligands H_4AAZTA and H_5DTPA (25 °C).

	H_4AAZTA 0.1 M KCl				H_5DTPA[a] 0.1 M KCl
	$\log K_{ML}$	$\log K^H_{MHL}$	$\log K^H_{MH_2L}$	$\log K^H_{MLH_{-1}}$	$\log K_{ML}$
Mg^{2+}	8.31 (0.01)	5.24 (0.06)	–	–	9.27
Ca^{2+}	12.76 (0.01)	3.34 (0.01)	–	–	10.75
Sr^{2+}	9.88 (0.01)	4.80 (0.05)	–	–	9.79
Mn^{2+}	15.44 (0.01)	2.83 (0.03)	–	–	15.2
Cu^{2+}[b]	20.51 (0.03)	4.00 (0.01)	2.72 (0.01)	10.81 (0.01)	21.5
Zn^{2+}	18.01 (0.02)	3.87 (0.01)	2.36 (0.02)	11.25 (0.03)	18.6
Pb^{2+}[c]	19.84 (0.04)	3.22 (0.04)	2.50 (0.05)	–	18.8
Cd^{2+}[c]	17.94 (0.01)	3.25 (0.01)	2.05 (0.02)	–	19.0
La^{3+}	17.53 (0.02)	1.97 (0.08)	–	–	19.48
Ce^{3+}	18.62 (0.01)	1.47 (0.03)	–	–	20.5
Nd^{3+}	19.41 (0.01)	1.73 (0.02)	–	–	21.6
Eu^{3+}	19.93 (0.01)	1.91 (0.01)	–	–	22.39
Gd^{3+}	20.24 (0.01)	1.89 (0.01)	–	–	22.46
Dy^{3+}	20.39 (0.01)	1.52 (0.03)	–	–	22.82
Er^{3+}	20.78 (0.02)	1.25 (0.06)	–	–	22.74
Yb^{3+}	21.59 (0.03)	–	–	–	22.62
Lu^{3+}	21.85 (0.04)	–	–	–	22.44

[a] Ref. [19]. [b] Obtained by UV/Vis spectrophotometry. [c] 25 °C, 0.1 M KNO_3.

The protonation and stability constants of AAZTA complexes were calculated from the titration curves obtained at metal-to-ligand concentration ratios of 1:1. The best fit was obtained by using the model that includes the formation of ML, MHL and MH_2L species in equilibrium. The titration data of the H_4AAZTA ligand in the presence of Zn^{2+} and Cu^{2+} ions indicate a base-consuming process at pH > 9. This process can be interpreted by assuming the hydrolysis of the metal ion and the coordination of the OH^- ion according to Equation (5):

$$ML + H_2O \rightleftharpoons ML(OH)^- + H_3O^+$$
$$K_{MLH-1} = \frac{[ML(OH)^-][H_3O^+]}{[ML]} \tag{5}$$

Because of the high stability of the $[Cu(AAZTA)]^{2-}$ complex, the determination of the stability constant could not be carried out by pH potentiometry. The stability constant was thus determined by studying the equilibrium in the Cu^{2+}/DTPA/AAZTA system by UV/Vis spectrophotometry. The competition reaction [Eq. (6)] was studied in the pH range 7–9, in which only the species $[Cu(AAZTA)]^{2-}$ and $[Cu(DTPA)]^{3-}$ are present in the equilibrium.

$$[Cu(AAZTA)]^{2-} + H_xDTPA \rightleftharpoons [Cu(DTPA)]^{3-} + H_yAAZTA + (x-y)H^+ \tag{6}$$

Characteristic absorption spectra obtained for the systems Cu^{2+}/AAZTA, Cu^{2+}/DTPA, and Cu^{2+}/AAZTA/DTPA are shown in Figure 2.

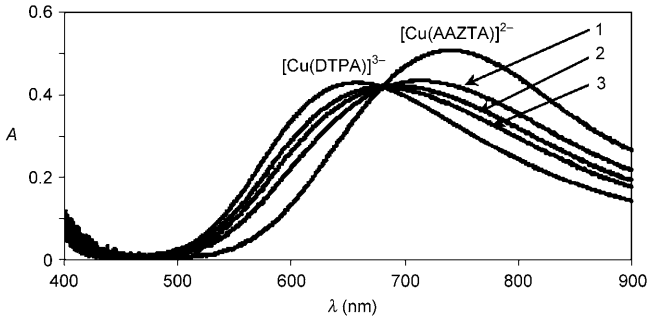

Figure 2. Absorption spectra of the $[Cu(DTPA)]^{3-}$ (0.005 M), $[Cu(AAZTA)]^{2-}$ (0.005 M) and $Cu^{2+}/AAZTA^{4-}/DTPA^{5-}$ systems ($[Cu^{2+}]=[AAZTA]=0.005$ M). 1) [DTPA] = 0.0025 M; 2) [DTPA] = 0.00375 M; 3) [DTPA] = 0.005 M. (pH 7.61, 0.1 M KCl, 25 °C).

The positions of the absorption band of $[Cu(AAZTA)]^{2-}$ and $[Cu(DTPA)]^{3-}$ differ considerably. The absorption maximum of $[Cu(AAZTA)]^{2-}$ is at 745 nm, whereas that of $[Cu(DTPA)]^{3-}$ is at 650 nm. In the pH range investigated, the isosbestic point in the spectra indicates the presence of two absorbing species, $[Cu(AAZTA)]^{2-}$ and $[Cu(DTPA)]^{3-}$. For the calculation of the stability constants, the protonation constants of DTPA (10.45, 8.60, 4.28, 2.64, and 2.03)[19] and of AAZTA (Table 2) and the stability constant of $[Cu(DTPA)]^{3-}$ ($\log K_{[Cu(DTPA)]}=21.38$)[19] were used. The stability constant of $[Cu(AAZTA)]^{2-}$, calculated with the program PSEQUAD,[30] is reported in Table 2. The protonation constants of $[Cu(AAZTA)]^{2-}$ (Table 2) were determined by the pH potentiometric titration of the complex from pH 2 to 6.

The pH potentiometric titrations were also carried out at a metal-to-ligand ratio of 2:1 to assess the possible formation of dinuclear complexes in the Zn^{2+}/AAZTA and Cu^{2+}/AAZTA systems. The protonation constants were calculated separately from the titration curves obtained at metal-to-ligand concentration ratios of 1:1 and 2:1 by using the model, which includes the formation of MHL and MH_2L species only. In the presence of an excess of Zn^{2+} or Cu^{2+} ions, the protonation constants (and the stability constant of the ZnL species) calculated were the same as those found at 1:1 concentration ratios, excluding the formation of dinuclear complexes.

The stability constants of the metal complexes formed with AAZTA (Table 2) are generally about one to two orders of magnitude lower than those of the corresponding complexes of DTPA. The $\log K_{ML}$ values determined for the Ca^{2+}, Sr^{2+}, Mn^{2+}, and Pb^{2+} complexes are similar or even higher than those of DTPA. This is surprising because both the denticity and the total basicity of AAZTA are clearly lower than those for DTPA. The stability constants of the Sr^{2+} complexes of AAZTA and DTPA are rather similar (Table 2), whereas the $\log K_{ML}$ value of $[Ca(AAZTA)]^{2-}$ is about two orders of magnitude higher than that of $[Ca(DTPA)]^{3-}$. This higher stability can be explained in terms of a good match between the size of the Ca^{2+} ion and the flexible cavity of the AAZTA ligand. The coordination of all the donor atoms to the smaller Mg^{2+} ion is not possible because of steric hindrance, while the Sr^{2+} ion is too large for a good match.

The stability constants of $[Ln(AAZTA)]^{-}$ complexes increase monotonously from La^{3+} to Lu^{3+} (Table 2), the trend is clearly recognizable in Figure 3. This behavior differs

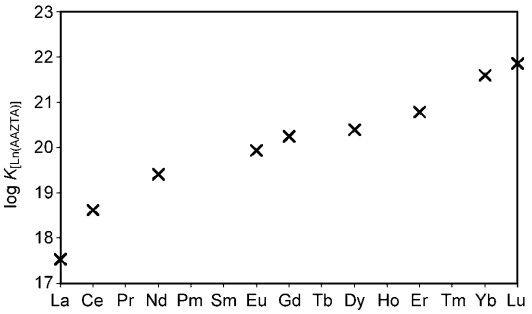

Figure 3. Plot of $\log K_{[Ln(AAZTA)]}$ versus lanthanoid.

from that found for the $[Ln(DTPA)]^{2-}$ complexes, which have $\log K_{ML}$ values that increase from La^{3+} to Dy^{3+}, then remain practically constant for the heavier lanthanoids with a slight decrease at the end of the series.[19] On the other hand, the stability constants of the Ln^{3+} complexes formed with AAZTA are lower than those of $[Ln(DTPA)]^{2-}$, but the differences between the $\log K_{LnL}$ values significantly decreases in the second half of the lanthanoid series. These data clearly indicate the role of the coordination cage of the ligand on the trend of $\log K_{ML}$ values across the lanthanoid series and the presence of an optimal size match for the Lu^{3+} ion.

The stability constants of the complexes of AAZTA with Zn^{2+}, Cd^{2+}, and Cu^{2+} (ions with a coordination number of six or below) are somewhat lower, approximately by one $\log K$ unit, than those of DTPA. This is probably the result of the less favorable size match between smaller metal ions and the coordination cage of AAZTA, which is less flexible than that of DTPA. Moreover, AAZTA can coordinate the larger Pb^{2+} and Mn^{2+} ions (which often have a coordination number of seven) by all of its donor atoms, thus leading to relatively larger stability constants.

The complexes formed with AAZTA, similarly to those of DTPA, can be protonated at lower pH values and the protonation constants have been determined by pH potentiometry (Table 2). For complexes formed with smaller metal ions (Zn^{2+}, Cd^{2+}, Cu^{2+}, but also Pb^{2+}), two protonation constants could be determined. In these complexes there is probably one noncoordinated donor atom (a carboxylate oxygen atom) protonated at pH values around 3–5. At lower pH values another oxygen atom can be protonated. The complexes of Mn^{2+}, Ca^{2+}, Sr^{2+}, and Ln^{3+} ions form only one protonated complex and the $\log K_{MHL}$ values are generally about 2–3, indicating the protonation of a carboxylate group.

Transmetalation kinetics of [Gd(AAZTA)]$^-$: The complexes of Gd^{3+}, used as MRI contrast agents, must have high kinetic inertness because the products of their dissociation, that is, the free Gd^{3+} and the ligand, are toxic. Nowadays it has been realized that, in the in vivo applications of Gd^{3+} complexes, the kinetic stability is even more important that the absolute value of the stability constant.[23,24,25] Body fluids are very complex systems and the study of the in vivo rate of dissociation reactions of Gd^{3+} complexes would be difficult. The results of in vitro studies may, however, provide important information concerning the kinetic behavior of the complexes under in vivo conditions. The kinetic stabilities of complexes are characterized either by the rates of their dissociation measured in 0.1 M HCl or by the rates of the transmetalation reaction, occurring in solutions with Zn^{2+} and Cu^{2+} or Eu^{3+}.[24–26] For a direct comparison of the kinetic properties of $[Gd(AAZTA)]^-$ and $[Gd(DTPA)]^{2-}$, the same method and identical conditions were used as those reported in previous work on $[Gd(DTPA)]^{2-}$.[25] The rates of the transmetalation reactions [Eq. (7), in which M^{n+} = Cu^{2+} or Eu^{3+}] were studied by spectrophotometry with the use of Cu^{2+} and Eu^{3+} as exchanging metal ions:

$$[Gd(AAZTA)]^- + M^{n+} \rightleftharpoons [M(AAZTA)]^{n-4} + Gd^{3+} \qquad (7)$$

In the presence of an excess of the exchanging ion, the transmetalation can be treated as a pseudo-first-order process and the rate of reactions can be expressed with Equation (8), in which k_{obs} is a pseudo-first-order rate constant and $[GdL]_{tot}$ is the total concentration of the complex.

$$-\frac{d[GdL]_{tot}}{dt} = k_{obs}[GdL]_{tot} \qquad (8)$$

The rates of the transmetalation reactions have been studied at different concentrations of the exchanging ions in the pH range 3.3–5.3. The rate constants k_{obs} obtained are presented in Figure 4 and as a function of the concentration of the exchanging ions and the concentration of H^+ ions (Figures S1 and S2 in the Supporting Information).

As it can be seen in Figure 4, the k_{obs} values exhibit a similar dependence in the reactions with the participation of Cu^{2+} and Eu^{3+}. The k_{obs} values increase upon increasing concentration of H^+ (particularly at lower concentrations of Cu^{2+} or Eu^{3+}) and also upon increasing concentrations of Cu^{2+} or Eu^{3+} at pH > 4.5. The increase in the k_{obs} values with increasing concentration of H^+ can be interpreted in terms of the relatively slow proton-assisted dissociation of $[Gd(AAZTA)]^-$, followed by a fast reaction between the free ligand and the exchanging metal ions Cu^{2+} or Eu^{3+}. The dependence of k_{obs} on the concentration of H^+ can be expressed as a first-order function of the H^+ concentration itself indicating that the exchange can take place by proton-independent [Eq. (9)] and proton-assisted [Eq. (10)] pathways. The proton-assisted dissociation of $[Gd(AAZTA)]^-$ can be explained by the equilibrium formation of a protonated [Gd(HAAZTA)] complex, which slowly dissociates and the free ligand rapidly reacts with the exchanging metal ions.

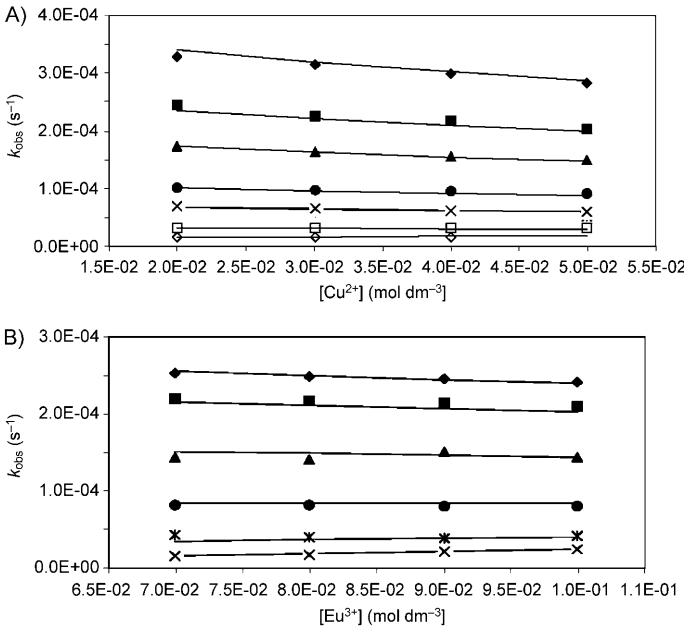

Figure 4. A) Plots of k_{obs} versus Cu^{2+} concentration for the reaction between $[Gd(AAZTA)]^-$ (0.001 M) and Cu^{2+} (pH 3.39 (◆), pH 3.56 (■), pH 3.71 (▲), pH 3.95 (●), pH 4.13 (×), pH 4.14 (*), pH 4.49 (□), and pH 4.82 (◇); 25 °C, 1.0 M KCl). B) Plots of k_{obs} versus Eu^{3+} concentration for the reaction between $[Gd(AAZTA)]^-$ (0.001 M) and Eu^{3+} (pH 3.35 (◆), pH 3.44 (■), pH 3.59 (▲), pH 3.90 (●), pH 4.21 (*) and pH 4.52 (×); 25 °C, 1.0 M KCl).

$$[Gd(AAZTA)]^- \xrightarrow{k_0} Gd^{3+} + H_xAAZTA \qquad (9)$$

$$[Gd(HAAZTA)] \xrightarrow{k_{GdHL}} Gd^{3+} + H_xAAZTA \qquad (10)$$

The increase in the rate of the exchange reactions with increasing Cu^{2+} or Eu^{3+} concentrations indicates that the reaction can take place with the direct attack of the exchanging metal ion on the complex via the formation of a dinuclear intermediate. In the case of the $[Ln(DTPA)]^{2-}$ complexes, the formation of homo- and heterodinuclear complexes were detected by ^{1}H NMR spectroscopy.[27] The formation of the dinuclear $[\{Lu(AAZTA)\}Cu]^+$ complex has also been observed by ^{1}H NMR spectroscopy in the presence of a large excess of the Cu^{2+} ion. The ^{1}H NMR spectra of the $[Lu(AAZTA)]^-$ in the presence and absence of Cu^{2+} are presented in Figure 5.

The chemical shifts and the line width of the ^{1}H NMR signals of $[Lu(AAZTA)]^-$ complex (2 and 3 in Figure 5) display significant changes in the presence of the Cu^{2+} ion (the ^{1}H NMR spectrum of $[Cu(AAZTA)]^{2-}$ could not be detected under these experimental conditions (4 in Figure 5) because the signals are too broad due to the long electronic relaxation time of Cu^{2+}). Since the rate of the ligand exchange between the $[Lu(AAZTA)]^-$ and $[Cu(AAZTA)]^{2-}$ complexes is slow on the NMR timescale, these changes can be interpreted with the direct interaction between the [Lu-

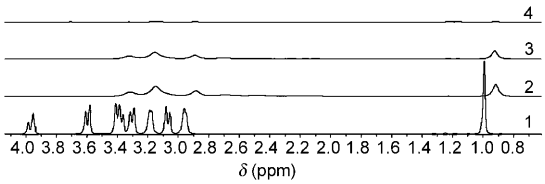

Figure 5. ^{1}H NMR spectra of the [Lu(AAZTA)]$^-$ (0.005 M) complex before (1) and 33 (2), 938 (3), and 2880 min (4) after the mixing with 0.25 M $CuCl_2$ (pH 4.2, 25 °C).

$(AAZTA)]^-$ complex and the paramagnetic Cu^{2+} ion, due to the formation of the dinuclear $[\{Lu(AAZTA)\}Cu]^+$ complex according to Equation (11):

$$Gd(AAZTA)^- + M^{n+} \underset{}{\overset{K^*_{GdLM}}{\rightleftharpoons}} [\{Gd(AAZTA)\}M]^{n-1}$$
$$K^*_{GdLM} = \frac{[\{Gd(AAZTA)M\}^{n-1}]}{[Gd(AAZTA)^-][M^{n+}]} \quad (11)$$

It can be assumed that in the dinuclear intermediate $([Gd(AAZTA)]M)^{n-1}$, the donor groups of AAZTA are slowly transferred from Gd^{3+} to the competing Cu^{2+} or Eu^{3+} ions stepwise [Eq. (12)].

$$(\{Gd(AAZTA)\}M]^{n-1} \rightarrow Gd^{3+} + [M(AAZTA)]^{n-4} \quad (12)$$

The trend in the k_{obs} values in Figure 4 shows that the increase in the concentration of Cu^{2+} and Eu^{3+} ions results in a slight decrease in the k_{obs} values at higher H^+ concentrations. This phenomenon can be interpreted by considering that the concentration of the dinuclear species increases with the increase in the concentration of the exchanging metal ion, when the concentration of the monoprotonated [Gd(HAAZTA)] decreases, resulting in the decrease of the rate of the proton-assisted dissociation of the complex ($[M^{n+}] \gg [H^+]$). Similar results were obtained in the exchange reactions of $[Cd(CDTA)]^{2-}$ (H_4CDTA = *trans*-diaminocyclohexane-*N*,*N*,*N*′,*N*′-tetraacetic acid) and [Ln(DTPA)] complexes.[25,28] By taking into account all the possible pathways, the rate of the transmetalation of $[Gd(AAZTA)]^-$ can be expressed by Equation (13), in which [GdHL] and [GdLM] are the concentrations of the protonated and dinuclear complexes, respectively:

$$-\frac{[GdL]_{tot}}{dt} = k_0[GdL] + k_{GdLH}[GdHL] + k_{GdLM}[GdLM] \quad (13)$$

Taking into account the total concentration of the complex ($[GdL]_{tot} = [GdL] + [GdHL] + [GdLM]$), the equation defining the protonation constant of the monoprotonated complex [Eq. (4)], and the stability constant of the dinuclear complex [Eqs. (11) and (8)], the pseudo-first-order rate constant can be expressed by Equation (14):

$$k_{obs} = \frac{k_0 + k_1[H^+] + k_3[M^{n+}]}{1 + K^H_{GdHL}[H^+] + K^*_{GdLM}[M^{n+}]} \quad (14)$$

The rate constants, k_0, $k_1 = k_{GdHL}K^H_{GdHL}$, and $k_3 = k_{GdLM}K^*_{GdLM}$ are characteristic for the reactions occurring by spontaneous, proton-assisted, and metal-assisted dissociation of $[Gd(AAZTA)]^-$, respectively. The rate, protonation, and stability constants have been calculated by fitting the k_{obs} values to Equation (14) and the values obtained are compared with the corresponding values of $[Gd(DTPA)]^{2-}$ in Table 3.

Table 3. Rate (k_i), stability (K^*_{GdLM}), and protonation (K^H_{GdHL}) constants characterizing the transmetalation of the complexes $[Gd(AAZTA)]^-$ and $[Gd(DTPA)]^{2-}$ (25 °C, 1.0 M KCl).

		k_1 [$M^{-1}s^{-1}$]	k_3 [$M^{-1}s^{-1}$]	K^H_{GdHL} [M^{-1}]	K^*_{GdLM} [M^{-1}]
$[Gd(AAZTA)]^-$	Cu^{2+}	1.05 ± 0.07	$(1.9 \pm 0.8) \times 10^{-4}$	233 ± 195	9 ± 2
	Eu^{3+}	1.18 ± 0.31	$(6.1 \pm 2.5) \times 10^{-4}$	271 ± 105	8 ± 5
$[Gd(DTPA)]^{2-}$[a]	Cu^{2+}	0.58	0.93	100	13
	Zn^{2+}	0.58	5.6×10^{-2}	100	7
	Eu^{3+}	0.58	4.9×10^{-4}	100	19

[a] Ref. [25].

The k_0 values obtained are very low and the error is very high, indicating the unimportance of the spontaneous dissociation of $[Gd(AAZTA)]^-$. The rate constants k_1, characterizing the proton-assisted dissociation of the complex, are somewhat higher than that measured for $[Gd(DTPA)]^{2-}$. On the basis of the solid-state structure of the $[Gd(AAZTA)]^-$ complex, the Ln^{3+} ion is coordinated by the three nitrogen atoms and four oxygen atoms.[22] For both complexes, the protonation probably occurs at a carboxylate group yielding an uncoordinated COOH group. The resulting protonated complex, however, appears to be unreactive, since the protonation/deprotonation step of the carboxylate group is fast and the COO^- group can again bind to the Gd^{3+} ion. Dissociation appears to be more likely if the proton is transferred to the nitrogen atom of the iminodiacetate fragment resulting in the relatively labile protonated intermediate in which the iminodiacetate moiety is free and the Gd^{3+} ion is weakly coordinated by the nitrogen and oxygen atoms of the DACHDA moiety only. The proton-assisted dissociation of $[Gd(DTPA)]^{2-}$ occurs similarly, but proton transfer to the central nitrogen atom is more difficult because the rate-determining step is presumably the cleavage of the coordination bond between the Gd^{3+} ion and the central nitrogen atom.[26]

The protonation constant of the $[Gd(AAZTA)]^-$ complex was also determined in separate experiments by pH potentiometric titration ($K^H_{GdL} = 77$ in Table 2). The protonation constants calculated from the kinetic data with Equation (14) (with quite high error limits) are higher, but this value is characteristic for the formation of the protonated complex, which is important in the rate-limiting step of the dissociation.

The rate constants obtained for the transmetalation reactions between $[Gd(AAZTA)]^-$ and the Cu^{2+} or Eu^{3+} ions are very similar and indicate that the role of the two metal

ions in the dissociation of $[Gd(AAZTA)]^-$ is comparable. The rate constant k_3^{Eu}, characterizing the efficiency of the Eu^{3+} attack on the complex is very similar for $[Gd(AAZTA)]^-$ and $[Gd(DTPA)]^{2-}$, whereas the k_3^{Cu} value is three orders of magnitude lower for $[Gd(AAZTA)]^-$ than for $[Gd(DTPA)]^{2-}$. These findings suggest that the coordination cage around the Gd^{3+} ion in the $[Gd(AAZTA)]^-$ complex is presumably robust, resulting in an enhanced hindrance for the transformation into the dinuclear intermediate. The stability constants of the dinuclear complexes are quite similar and the much lower k_3^{Cu} and k_3^{Eu} values for the $[Gd(AAZTA)]^-$ indicate the much lower kinetic activity of the dinuclear $[\{Gd(AAZTA)\}M]^{n-1}$ complexes.

By using the obtained dissociation rate constants, it is possible to compare the kinetic stabilities of the Gd^{3+} complexes at pH 7.4 and at various Cu^{2+} and Zn^{2+} concentrations, which are similar to those of the plasma. According to the plasma model developed by May et al., the concentrations of the exchangeable Cu^{2+} and Zn^{2+} ions are 1×10^{-6} and 1.6×10^{-5} M, respectively.[14] In the presence of Cu^{2+} and Zn^{2+}, the rate of the proton-, Cu^{2+}-, and Zn^{2+}-assisted dissociation of $[Gd(AAZTA)]^-$ and $[Gd(DTPA)]^{2-}$ can be expressed by Equation (15):

$$k_{obs}^{S} = k_1[H^+] + k_3^{Cu}[Cu^{2+}] + k_3^{Zn}[Zn^{2+}] \quad (15)$$

in which k_{obs}^{S} is a pseudo-first-order rate constant. The results of our kinetic studies, however, show that the importance of the metal-assisted dissociation for $[Gd(AAZTA)]^-$ is very low and, at the low Cu^{2+} and Zn^{2+} concentrations indicated above, their contribution is negligible (the importance of the Zn^{2+}-assisted transmetalation is generally lower than the Cu^{2+} assisted one[25,26]). By taking into account these considerations, for the reaction of $[Gd(AAZTA)]^-$, the terms $k_3^{Cu}[Cu^{2+}]$ and $k_3^{Zn}[Zn^{2+}]$ can be neglected and Equation (15) simplifies to $k_{obs}^{S} = k_1[H^+]$. The k_{obs}^{S}values calculated for $[Gd(AAZTA)]^-$, with the average of the k_1 values presented in Table 3, and also for $[Gd(DTPA)]^{2-}$, with the use of Equation (15), are shown in Table 4. By using the k_{obs}^{S} values, the half-lives of dissociation ($t_{1/2}$) can be calculated for $[Gd(AAZTA)]^-$ and $[Gd(DTPA)]^{2-}$ (Table 4).[25]

Table 4. Pseudo-first-order rate constants (k_{obs}^{S}) and half-life ($t_{1/2}$) for the dissociation of the complexes $[Gd(AAZTA)]^-$ and $[Gd(DTPA)]^{2-}$ at pH 7.4, $[Cu^{2+}]=1\times10^{-6}$ M and $[Zn^{2+}]=1\times10^{-5}$ M (25 °C, 1.0 M KCl).

	$10^6\times k_{obs}^{S}$ [s^{-1}]	$t_{1/2}$ [h]
$[Gd(DTPA)]^{2-}$[a]	1.51	127
$[Gd(AAZTA)]^-$	0.045	4337

[a] Ref. [25].

Comparison of the pseudo-first-order rate constants k_{obs}^{S} and the $t_{1/2}$ values calculated for $[Gd(AAZTA)]^-$ and $[Gd(DTPA)]^{2-}$ (Table 4) shows that $[Gd(AAZTA)]^-$ is much more inert than $[Gd(DTPA)]^{2-}$. If only the proton-assisted dissociation was taken into account (as it was in some earlier studies made in 0.1 M acid[24]), the pseudo-first-order rate constant ($k_{obs}^{S}=2.31\times10^{-8}\ s^{-1}$) and the half-lives of the dissociation ($t_{1/2}=8338$ h) would be somewhat more favorable for $[Gd(DTPA)]^{2-}$. The reactions between $[Gd(DTPA)]^{2-}$ and Cu^{2+} or Zn^{2+}, however, proceed much faster than the proton-assisted dissociation of the complex, so the transmetalation of $[Gd(DTPA)]^{2-}$ may occur by the reaction with Cu^{2+} or Zn^{2+} ions in body fluids and the proton-assisted dissociation of the complex is negligible. On the basis of these considerations, the complex $[Gd(AAZTA)]^-$ is expected to be more inert than $[Gd(DTPA)]^{2-}$ under physiological conditions.

Conclusion

The heptadentate chelating agent AAZTA can be regarded as a combination of the cyclic 1,4-diazacycloheptane-1,4-diacetate and the iminodiacetate ligands and has properties that are intermediate between the typical open-chain polyaminopolycarboxylates and the macrocyclic polyazapolycarboxylates. Considering its coordination ability, the complexation properties of AAZTA are comparable with those of DTPA. Due to the presence of the diazacycloheptane ring, AAZTA can form a cage-like coordination polyhedron around the metal ions to give a complex that is more rigid than that of DTPA, but more flexible than the cage formed by macrocyclic derivatives, such as DOTA. Thus, in the case of a favorable size match, AAZTA forms metal complexes of high stability with di- and trivalent metal ions. The AAZTA complexes of Ca^{2+} and Pb^{2+}, similarly to those of the macrocyclic DOTA, have significantly higher stability constants than those of DTPA. The stabilities of the AAZTA and DTPA complexes of Sr^{2+}, Mn^{2+}, and Zn^{2+} are comparable, whereas those containing Mg^{2+}, Cu^{2+}, Cd^{2+}, and Ln^{3+} ions form more stable complexes with DTPA than with AAZTA. In the complexes formed with the smaller metal ions, AAZTA is coordinated in a hexa- or pentadentate fashion, as indicated by the higher values of the protonation constants of complexes.

The $\log K_{ML}$ values of the $[Ln(AAZTA)]^-$ complexes monotonously increase, whereas the protonation constants of complexes decrease with increasing atomic number of the lanthanoids and because of the increase in the metal–ligand interactions; the protonation of $[Yb(AAZTA)]^-$ and $[Lu(AAZTA)]^-$ could not be detected.

The high thermodynamic stability shown by $[Gd(AAZTA)]^-$ (which is more than one order of magnitude higher than the previously reported value[11]) promotes the system into the group of Gd^{3+} chelates for in vivo applications in spite of its lower denticity. The rate of the proton-assisted dissociation of $[Gd(AAZTA)]^-$ is somewhat higher than that of $[Gd(DTPA)]^{2-}$, but it is of low importance at physiological pH. A much higher resistance against the attack of metal ions was also demonstrated by $[Gd(AAZTA)]^-$, so the rates of its transmetalation reaction with Cu^{2+} and presumably with other endogenous metal

ions are significantly lower than that of $[Gd(DTPA)]^{2-}$. The half-lives of dissociation of $[Gd(AAZTA)]^{-}$ and $[Gd(DTPA)]^{2-}$ near to physiological conditions, calculated with the kinetic data obtained by in vitro experiments, are 4337 and 127 h, respectively, indicating the higher kinetic stability of $[Gd(AAZTA)]^{-}$.

Overall, the high relaxivity, good stability, and kinetic inertness make $[Gd(AAZTA)]^{-}$ a reference structure for the development of a novel class of MRI contrast agents.

Experimental Section

Equilibrium measurements: The chemicals used for the experiments were of the highest analytical grade. The solutions of $LnCl_3$ were prepared from $LnCl_3{\cdot}xH_2O$ (x = 5–7) (Aldrich; 99.9%). The concentration of the solutions of $MgCl_2$, $CaCl_2$, $SrCl_2$, $MnCl_2$, $Pb(NO_3)_2$, $CdCl_2$, $ZnCl_2$, $CuCl_2$, and $LnCl_3$ were determined by complexometric titration with standardized Na_2H_2EDTA and Xylenol Orange ($ZnCl_2$, $Pb(NO_3)_2$, $CdCl_2$, $LnCl_3$), murexid ($CuCl_2$), Patton & Reeder ($CaCl_2$), Methylthymolblue ($SrCl_2$), and Eriochrome Black T ($MgCl_2$, $MnCl_2$) as indicators. The concentration of the H_4AAZTA was determined by pH potentiometric titrations in the presence and absence of a large (40-fold) excess of $CaCl_2$.

The protonation and the stability constants of some metal complexes formed with AAZTA ligand were determined by pH potentiometric titration. The metal-to-ligand concentration ratios were 1:1, but for the Cu^{2+} and Zn^{2+} complexes, titrations were also made at a metal-to-ligand ratio of 2:1 (the concentration of the ligand was generally 0.002 M).

For the pH measurements and titrations, a CRISON micro pH 2002 pH meter, a CRISON micro BU2030 autoburette, and a Metrohm-6.0233.100 combined electrode were used. Equilibrium measurements were carried out at a constant ionic strength (0.1 or 1.0 M KCl, KNO_3, and TMACl) in 10 mL samples at 25 °C; the solutions were stirred, and N_2 was bubbled through them. The titrations were made in the pH range 1.7–11.7. For the calibration of the pH meter, buffer standard solution, color-coded "pink" (pH 4.010) (Fluka) and buffer standard solution, color-coded "yellow" (pH 7.000) (Fluka) were used. For the calculation of the concentration of H^+ from the measured pH values, the method proposed by Irving et al. was used.[29] A 0.01 M aqueous solution of HCl or a 0.01 M aqueous solution of HNO_3 was titrated with the standardized aqueous solution of KOH or tetramethylammonium (TMAOH). The differences between the measured and calculated pH values were used to obtain the H^+ concentration from the pH values, measured in the titration experiments.

Spectrophotometric measurements were carried out on the absorption band of $[Cu(AAZTA)]^{2-}$ and $[Cu(DTPA)]^{3-}$ in the wavelength range 400–900 nm. Three series of samples were prepared containing [DTPA] = 2.5×10^{-3}, 3.75×10^{-3}, or 5×10^{-3} M, [AAZTA] = 5×10^{-3} M, [Cu^{2+}] = 5×10^{-3} M and 0.1 M KCl. In each series, five samples (3×5×5 mL) were prepared with different pH values in the pH range 7.3–8.7. The samples were kept at 25 °C for about two weeks in order for equilibrium to be attained (the time needed to reach the equilibrium was previously determined by spectrophotometry). The molar absorptivities of $[Cu(AAZTA)]^{2-}$ and $[Cu(DTPA)]^{3-}$ at 12 different wavelengths (500, 540, 580, 620, 660, 700, 740, 760, 780, 820, 840, and 860 nm) were determined by recording the spectra of solutions with concentrations of 1.5×10^{-3}, 3×10^{-3}, 5×10^{-3}, and 7×10^{-3} M (pH 7.61). For the calculation of the equilibrium data, the absorbance values were measured at 12 wavelength values (500, 540, 580, 620, 660, 700, 740, 760, 780, 820, 840, and 860 nm). The spectrophotometric measurements were made with the use of a Cary 1E spectrophotometer in 1.0 cm cells at 25 °C.

The protonation and stability constants were calculated with the program PSEQUAD.[30]

NMR experiments: ^{1}H NMR measurements were performed with either a JEOL Eclipse Plus 400 or a Bruker Avance 600 spectrometer with a 5 mm probe at 298 K. The protonation process of the H_4AAZTA ligand was followed by ^{1}H NMR spectroscopy. For these experiments, a 0.01 M solution of the ligand in D_2O was prepared. The pH was adjusted by stepwise addition of a solution of KOH and HCl (both prepared in D_2O). The pH values reported for the ligand were corrected for the deuterium effect by using the relationship pD = pH + 0.4.[31] The calculations were performed with the computer program Micromath Scientist, version 2.0 (Salt Lake City, UT, USA).

Metal-exchange kinetics: The kinetic stability of $[Gd(AAZTA)]^{-}$ was characterized by the rates of the exchange reactions taking place between the $[Gd(AAZTA)]^{-}$ and Eu^{3+} or Cu^{2+} ions. The exchange reactions with Eu^{3+} or Cu^{2+} were studied by spectrophotometry, following the formation of the Eu^{3+} or Cu^{2+} complexes at 250 or 330 nm with a Cary 1E spectrophotometer. The concentration of the $[Gd(AAZTA)]^{-}$ complex was 1×10^{-3} M, whereas the concentrations of the Cu^{2+} and Eu^{3+} ions were higher (20–50:1 and 70–100:1, respectively) to guarantee pseudo-first-order conditions. The temperature was maintained at 25 °C and the ionic strength of the solutions was kept constant, 1.0 M for KCl. The exchange rates were studied in the pH range 3.1–5.2. To keep the pH values constant, 1,4-dimethylpiperazine (pH range 3.1–4.1) and *N*-methylpiperazine (pH range 4.1–5.2) buffers (0.02 M) were used. The pseudo-first-order rate constants (k_{obs}) were calculated by fitting the absorbance data to Equation (16):

$$A_t = (A_0 - A_p)e^{-k_{obs}t} + A_p \qquad (16)$$

in which A_t, A_0, and A_p are the absorbance values at time t, the start of the reaction, and at equilibrium, respectively.

Acknowledgements

We gratefully acknowledge financial support from MUR (FIRB and PRIN projects), Eu-NoE EMIL, and DIMI. The work was carried out under the collaborative scheme of EU-COST D38 action.

[1] a) J. C. Bünzli, G. R. Choppin, *Lanthanide Probes in Life, Chemical and Earth Sciences*, Elsevier, Amsterdam, **1989**; b) J. Rocha, L. D. Carlos, *Curr. Opin. Solid State Mater. Sci.* **2003**, *7*, 199–205; c) D. Parker, *Chem. Soc. Rev.* **2004**, *33*, 156–165; d) J. C. Bünzli, C. Piguet *Chem. Soc. Rev.* **2005**, *34*, 1048–1077; e) S. Pandya, J. Yu, D. Parker, *Dalton Trans.* **2006**, 2757–2766.

[2] P. A. Rinck, *Magnetic Resonance in Medicine*, ABW, Berlin, **2003**.

[3] a) P. Caravan, J. J. Ellison, T. J. McMurry, R. B. Lauffer, *Chem. Rev.* **1999**, *99*, 2293–2352; b) S. Aime, M. Botta, E. Terreno, *Gd^{III}-based Contrast Agents for MRI in Advances in Inorganic Chemistry, Vol. 57* (Eds.: R. van Eldik, I. Bertini), Elsevier, San Diego **2005**, pp. 173–237; c) S. Aime, S. Geninatti Crich, E. Gianolio, G. B. Giovenzana, L. Tei, E. Terreno, *Coord. Chem. Rev.* **2006**, *250*, 1562–1579.

[4] a) L. Thunus, R. Lejeune, *Coord. Chem. Rev.* **1999**, *184*, 125–155; b) F. Rosch, E. Forssell-Aronsson in *Metal Ions in Biological Systems, Vol. 42* (Eds.: A. Sigel, H. Sigel), Marcel Dekker, New York, **2004**, pp. 77–108.

[5] a) H. S. Thomsen, S. K. Morcos, P. Dawson, *Clin. Radiol.* **2006**, *61*, 905–906; b) I. Erguen, K. Keven, I. Uruc, Y. Ekmeci, B. Canbakan, I. Erden, O. Karatan, *Nephrol. Dial. Transplant.* **2006**, *21*, 697–700; c) C. Thakral, J. Alhariri, J. L. Abraham, *Contrast Media Mol. Imaging* **2007**, *2*, 199–205.

[6] J. Xu, S. J. Franklin, D. W. Whisenhunt, Jr., K. N. Raymond, *J. Am. Chem. Soc.* **1995**, *117*, 7245–7246.

[7] S. Hajela, M. Botta, S. Giraudo, J. Xu, K. N. Raymond, S. Aime, *J. Am. Chem. Soc.* **2000**, *122*, 11228–11229.

[8] D. M. J. Doble, M. Botta, J. Wang, S. Aime, A. Barge, K. N. Raymond, *J. Am. Chem. Soc.* **2001**, *123*, 10758–10759.

[9] P. Caravan, J. C. Amedio, Jr., S. U. Dunham, M. T. Greenfield, N. J. Cloutier, S. A. McDermid, M. Spiller, S. G. Zech, R. J. Looby, A. M. Raitsimring, T. J. McMurry, R. B. Lauffer, *Chem. Eur. J.* **2005**, *11*, 5866–5874.
[10] a) J. B. Livramento, C. Weidensteiner, M. I. M. Prata, P. R. Allegrini, C. F. G. C. Geraldes, L. Helm, R. Kneuer, A. E. Merbach, A. C. Santos, P. Schmidt, É. Tóth, *Contrast Media Mol. Imaging* **2006**, *1*, 30–39; b) J. B. Livramento, A. Sour, A. Borel, A. E. Merbach, É. Tóth, *Chem. Eur. J.* **2006**, *12*, 989–1003.
[11] S. Aime, L. Calabi, C. Cavallotti, E. Gianolio, G. B. Giovenzana, P. Losi, A. Maiocchi, G. Palmisano, M. Sisti, *Inorg. Chem.* **2004**, *43*, 7588–7590.
[12] a) E. Gianolio, G. B. Giovenzana, D. Longo, I. Longo, I. Menegotto, *Chem. Eur. J.* **2007**, *13*, 5785–5797; b) S. Geninatti Crich, S. Lanzardo, D. Alberti, S. Belfiore, A. Ciampa, G. B. Giovenzana, C. Lovazzano, R. Pagliarin, *Neoplasia* **2007**, *9*, 1046–1056.
[13] E. Gianolio, G. B. Giovenzana, A. Ciampa, S. Lanzardo, D. Imperio, S. Aime, *ChemMedChem* **2008**, *3*, 60–62.
[14] P. M. May, D. R. Williams, P. W. Linder, *J. Chem. Soc. Dalton Trans.* **1977**, 588–595.
[15] G. Berthon, R. Hacht, M. Blais, P. M. May, *Inorg. Chim. Acta* **1986**, *125*, 219–227.
[16] W. P. Cacheris, S. C. Quay, S. M. Rocklage, *Magn. Reson. Imaging* **1990**, *8*, 467–481.
[17] G. E. Jackson, S. Wynchank, M. Woudenberg, *Magn. Reson. Med.* **1990**, *16*, 57–66.
[18] É. Tóth, L. Helm, A. E. Merbach in: *The Chemistry of Contrast Agents in Medical Magnetic Resonance Imaging* (Eds.: É. Tóth, A. E. Merbach), Wiley, Chichester, **2001**, 243–279.
[19] A. E. Martell, R. M. Smith, *Critical Stability Constants, Vol. 4*, Plenum, New York, **1974**.
[20] J. R. Ascenso, M. A. Santos, J. J. R. F. da Silva, M. C. T. A. Vaz, M. G. B. Drew, *J. Chem. Soc. Perkin Trans. 2* **1990**, 2211–2218.
[21] J. L. Sudmeier, C. N. Reilley, *Anal. Chem.* **1964**, *36*, 1698–1706.
[22] S. Aime, G. Bombieri, C. Cavallotti, G. B. Giovenzana, D. Imperio, N. Marchini, *Inorg. Chim. Acta* **2008**, *361*, 1534–1541.
[23] R. B. Lauffer, *Magn. Reson. Q.* **1992**, *6*, 65–84.
[24] P. Wedeking, K. Kumar, M. F. Tweedle, *Magn. Reson. Imaging* **1992**, *10*, 641–648.
[25] L. Sarka, L. Burai, E. Brucher, *Chem. Eur. J.* **2000**, *6*, 719–724.
[26] L. Sarka, L. Burai, R. Kiraly, L. Zekany, E. Brucher, *J. Inorg. Biochem.* **2002**, *91*, 320–326.
[27] J. A. Peters, *Inorg. Chem.* **1988**, *27*, 4686–4691.
[28] G. F. Smith, D. W. Margerum, *Inorg. Chem.* **1969**, *8*, 135–138.
[29] H. M. Irving, M. G. Miles, L. Pettit, *Anal. Chim. Acta* **1967**, *38*, 475–488.
[30] L. Zékány, I. Nagypál in *Computational Method for Determination of Formation Constants* (Ed.: D. J. Legett), Plenum, New York, **1985**, pp. 291–353.
[31] P. K. Glasoe, F. A. Long, *J. Phys. Chem.* **1960**, *64*, 188–190.

Received: September 2, 2008
Published online: January 7, 2009

